Original Article

Effects of liver X receptor in O3-induced airway inflammation and remodeling in mice

Fenfang Yu[1#], Jiyong Ma[1#], Ke Xu[2#], Yu Tang[3], Bining Wu[2], Wei Gu[1], Ying Shi[1]

[1]Department of Respiratory Medicine, Nanjing First Hospital, Nanjing Medical University, Nanjing, China; [2]Department of Respiratory Medicine, Nanjing Yuhua Hospital, Yuhua Branch of Nanjing First Hospital, Nanjing, China; [3]Department of Thoracic Surgery, Nanjing First Hospital, Nanjing Medical University, Nanjing, China

Contributions: (I) Conception and design: Y Shi, W Gu, B Wu; (II) Administrative support: W Gu, B Wu; (III) Provision of study materials or patients: F Yu, J Ma; (IV) Collection and assembly of data: K Xu; (V) Data analysis and interpretation: Y Tang; (VI) Manuscript writing: All authors; (VII) Final approval of manuscript: All authors.

[#]These authors contributed equally to this work.

Correspondence to: Ying Shi, PhD; Wei Gu, MD. Department of Respiration Medicine, Nanjing First Hospital, Nanjing Medical University, No. 68, Changle Road, Qinhuai District, Nanjing 210006, China. Email: sykxss@163.com; guw2001@126.com. Bining Wu, MD. Department of Respiratory Medicine, Nanjing Yuhua Hospital, Yuhua Branch of Nanjing First Hospital, No. 96 Yuhua Road, Yuhuatai District, Nanjing 210012, China. Email: wubining @126.com.

Background: The current clinical treatment of chronic obstructive pulmonary disease (COPD) mainly uses drugs to improve symptoms, but these drugs cannot reverse the progression of the disease and the pathological changes in lung tissue. This study aimed to investigate the effects and mechanisms of Liver X receptors (LXRs) in ozone (O3)-induced airway inflammation and remodeling in mice.

Methods: Wild mice and LXR deficient mice were exposed to O3 twice a week for 6 weeks. Some wild mice were intraperitoneally injected with T0901317 (a LXR agonist) before O3 exposure. Wild mice were exposed to ambient air and intraperitoneally injected with normal saline (NS) as control group. The lung tissues and bronchoalveolar lavage fluid (BALF) were collected to evaluate airway inflammation, airway remodeling and lipid disorder.

Results: After O3 exposure, LXR deficient mice showed severe airway inflammation and airway remodeling compared with the wild mice. There were a lot of foamy macrophages appeared in BALF of LXR deficient mice. The inflammatory proteins such as myeloid differentiation primary response protein 88 (MyD88) and interleukin-1 receptor-associated kinase (IRAK) in the lung tissues of LXR deficient mice were significantly increased compared with the wild mice. In wild mice exposed to O3, T0901317 treatment can alleviate airway inflammation, airway remodeling and foamy macrophages in BALF. And MyD88 and IRAK expression in lung tissue were also attenuated by T0901317 treatment.

Conclusions: LXRs play protective roles in O3-induced lipid accumulation, airway inflammation and airway remodeling.

Keywords: Liver X receptor (LXR); O3; airway inflammation; airway remodeling

Submitted Nov 29, 2023. Accepted for publication Jun 21, 2024. Published online Aug 14, 2024.
doi: 10.21037/jtd-23-1820
View this article at: https://dx.doi.org/10.21037/jtd-23-1820

Introduction

Ozone (O3) is a common air pollutant that can cause various adverse health issues in humans, particularly respiratory diseases. Inhalation of O3 can result in airway inflammation and decreased lung function. Clinical studies have confirmed that high-level O3 exposure can exacerbate symptoms and increase hospitalization rate in patients with asthma (1) and chronic obstructive pulmonary disease

(COPD) (2). Previous studies have demonstrated that chronic O3 exposure can induce an emphysema-like model in mice, characterized by features such as emphysema, neutrophilic inflammation, and elevated cytokine levels (3-5). O3 has been employed in various animal species to induce lung inflammation and airway remodeling (6,7). However, the precise mechanisms underlying O3-mediated lung injury remain unclear. Inhaled O3 readily reacts with lung lining fluid, which is distributed throughout the airway, forming a lipid ozonation product (LOP), which may contribute to the pro-inflammatory effect of O3. Within the human airway epithelium, LOP can activate pro-inflammatory factors, such as interleukin-6 (IL-6) and interleukin-8 (IL-8) (8,9).

Liver X receptors (LXRs), part of the nuclear receptor superfamily, are transcription factors with two isoforms: α (NR1H3) and β (NR1H2) (10). When bound to natural ligands, such as oxysterols and desmosterol (11) or synthetic ligands, such as T0901317 (12), LXRs regulate the transcription of genes related to cholesterol efflux and inflammation mediated by macrophage. Cholesterol is a crucial component of cells and macrophages are the primary inflammatory cells in the alveolar microenvironment. Thus, we hypothesized that LXRs play a significant role in O3-induced lipid accumulation and airway injury. In this study, we utilized LXR agonist and LXR-deficient mice to investigate the effect and mechanisms of LXRs following O3 exposure. We present this article in accordance with the ARRIVE reporting checklist (available at https://jtd.amegroups.com/article/view/10.21037/jtd-23-1820/rc).

Highlight box

Key findings

- Liver X receptors (LXRs) play protective roles in ozone (O3)-induced airway inflammation and airway remodeling in mice.

What is known and what is new?

- Previous research revealed the impact of LXR agonists *in vivo* following O3 exposure, and the susceptibility to O3-induced acute inflammation (3-hour exposure) was only observed in LXRα$^{-/-}$.
- We confirmed the protective role of LXR in O3-induced airway inflammation and remodeling through LXR agonists and LXR gene knockout.

What is the implication, and what should change now?

- Our research provides an experimental basis for the study of drug targets for ozone-induced airway inflammation and airway remodeling, and we need to further study its mechanism.

Methods

A protocol including the research question, key design features, and analysis plan was prepared before the study without registration.

Experimental animal

Animals were provided with unlimited sterile tap water and standard rodent feed at a temperature of 22±24 ℃ and a relative humidity of 50%±60% within a specific pathogen-free biosafety Level 3 facility. The animals involved in this experiment consisted of wild mice and gene knockout mice (LXRα$^{-/-}$, LXRβ$^{-/-}$, LXRα$^{-/-}$/β$^{-/-}$). The LXR-deficient mice, with a C57BL/6J background, were generated by the Nanjing University-Nanjing Biomedical Research Institute. LXRα$^{-/-}$/β$^{-/-}$ mice were bred from LXRα$^{-/-}$ mice and LXRβ$^{-/-}$ mice using Clustered Regularly Interspaced Short Palindromic Repeats (CRISPR)/Cas9 technique, where specifically designed and transcribed gRNA were used *in vitro*. Cas9 protein and (guide ribonucleic acid) gRNA was concurrently injected into fertilized mouse eggs. Cas9 protein, guided by gRNA, bound to the target site, inducing deoxyribonucleic acid (DNA) double-strand breaks, ultimately resulting in the deletion of base sequences at the target site and the removal of specific genes. The animal experiments were performed under a project license (No. SYXK [Su] 2016-0006) granted by the Animal Experiment Center of Nanjing First Hospital Affiliated to Nanjing Medical University, in compliance with guidelines established by the institution's Animal Care and Use Committee for the care and use of animals. All animal procedures were conducted under anesthesia (pentobarbital sodium at a concentration of 1%), with every effort made to minimize animal discomfort.

Exposure to O3 and LXR agonist treatment

Mice were randomly divided into six groups (n=5 per group):

(I) Control group: wild mice were exposed to ambient air and administrated normal saline (NS);
(II) O3 group: wild mice were exposed to O3 and administrated NS;
(III) T0901317 group: wild mice were exposed to O3 and administrated LXR agonist T0901317;
(IV) LXRα$^{-/-}$ group: LXRα$^{-/-}$ mice were exposed to O3 and administrated NS;

(V) LXRβ$^{-/-}$ group: LXRβ$^{-/-}$ mice were exposed to O3 and administrated NS;
(VI) LXRα$^{-/-}$/β$^{-/-}$ group: LXRα$^{-/-}$/β$^{-/-}$ mice were exposed to O3 and administrated NS.

With the exception of the control group, mice were exposed to O3 produced by an Ozonizer (Sander Ozonizer, Germany) mixed with air at a concentration of 2.5 parts per million (ppm) in a glass container for 3 hours, twice a week for 6 weeks. Continuous monitoring of O3 concentration using O3 probe (Analytical Technology, UK). T0901317 (Sigma Aldrich, USA) was dissolved in dimethyl sulfoxide (DMSO) to prepare a 100 mg/mL stock solution. One hour before O3 exposure, T0901317 (30 mL/kg) was administered intraperitoneally. This dose of T0901317 has been shown to activate ATP-binding cassette transporter A1 (ABCA1) and has an inhibitory effect on inflammatory diseases *in vivo* (13,14). Control animals were exposed to ambient air. Mice were euthanized 24 hours after the last O3 exposure.

Bronchoalveolar lavage fluid (BALF) collection

Mice were euthanized, and tracheotomy was performed. Ice-cold PBS (0.5 mL) was instilled into the lungs and the procedure was repeated three times, and BALF was retrieved. Return volume was recorded and was consistently >80% of the instilled volume. Total cell counts and differential cell counts were determined from the slides stained with Wright-Giemsa stain (KeyGEN BioTECH, Nanjing, China) using an optical microscope (Olympus Optical, Tokyo, Japan). A minimum of 200 cells per mouse were counted under ×400 magnification, and cells were classified as macrophages, lymphocytes, or neutrophils based on their standard morphological characteristics. The BALF supernatant was collected and stored at −80 ℃ for future biochemical analysis.

Enzyme linked immunosorbent assay (ELISA)

Levels of IL-6, tumor necrosis factor-α (TNF-α), and matrix metalloproteinase 9 (MMP9) in BALF were quantified using ELISA kits from CUSABIO, China, following the manufacturer's instructions.

Histology and Masson trichrome staining

After collecting the BALF samples, the left lung tissue was fixed in 10% (v/v) neutral buffed formalin. Subsequently, the tissue was embedded in paraffin, sectioned to a thickness of 5 μm, and stained with hematoxylin and eosin (HE) solution to assess the inflammatory response. Quantitative analysis was conducted following previously described methods (15,16). Peribronchial inflammation severity was assessed on lung images stained with HE, scored from 0 to 5, where 0= no cells, 1= a few cells, 2= a ring of cells one layer deep, 3= a ring of cells two layers deep, 4= a ring of cells three to four layers deep, and 5= a ring more than four cell layers deep. Additionally, Masson Trichrome staining was employed to detect collagen deposition, following the recommended standard protocol provided by the manufacturer. All histological assessments were conducted in a double-blinded manner under 400× magnification. The results were quantified by calculating the average of each airway.

Mean linear intercept (Lm)

The HE-stained tissues were examined under an optical microscope at a magnification of 200×, and ten random peripheral visual fields were selected from each section. The section images were imported into Photoshop, where a reference line was drawn passing through the central positive region of the image (while avoiding the areas containing airways and blood vessels as much as possible). The number of alveolar space (n) intersected by these two-reference line was counted, and the total length of the reference line (L) was measured. The average alveolar diameter (Lm) was then calculated using the formula Lm = L/N. This value serves as an indicator of the average alveolar size and reflects the alveolar damage (5).

Immunostaining for α-smooth muscle actin (α-SMA) and MMP9

The paraffin-embedded tissue sections were initially dewaxed in water. Subsequently, they were immersed in a 3% H_2O_2 solution at room temperature for 10 minutes to quench the activity of the endogenous peroxidase. Afterward, they were thoroughly rinsed with distilled water and soaked in phosphate buffered saline (PBS) for 5 minutes, repeating this step twice. Following this, the sections were blocked with 5% normal goat serum (diluted with PBS) and left to incubate at room temperature for 10 minutes, after which the excess serum was drained without further washing.

Next, primary antibodies against MMP9 (Servicebio GB11132) and α-SMA (Servicebio GB13044) were applied to the sections. The section was incubated either for two

hours at 37 ℃ or overnight at 4 ℃. Subsequently, the sections were rinsed with PBS for 5 minutes, repeating this step three times.

Afterward, an appropriate horseradish peroxidase (HRP)-labeled secondary antibody working solution (Servicebio GB23303) was applied to the sections, and they were incubated at 37 ℃ for 30 minutes. The sections were once again rinsed with PBS for 5 minutes, repeating this step three times. Following this, an adequate amount of horseradish enzyme-labeled streptomycin working solution was applied to the sections, and they were incubated at 37 ℃ for 30 minutes. The sections were then rinsed with PBS for 5 minutes, repeating this step three times.

Finally, the chromogenic agent (DAB) was applied to the section for 8 minutes. Subsequent steps included thorough flushing, re-staining, dehydration, clearing, and sealing with tap water. The results were quantified based on the averaged optical density within the airway.

Oil red O assay

BALF was collected from mice and plated on slides with Dulbecco's modified eagle medium (DMEM). The cells were incubated for four hours to allow for adhesion, washed three times with sterile PBS, and fixed with 4% paraformaldehyde fixative solution for 20 minutes. Subsequently, the cells were rinsed three times with distilled water, and the slides were briefly immersed in 60% isopropanol for 15 seconds.

Next, Oil Red O stain solution (KeyGEN BioTECH, Nanjing, China) was applied to each slide, and the slides were incubated for 30 minutes at 37 ℃. After 30 minutes, the slides were briefly washed with 60% isopropanol for 15 seconds (with precise timing control). Following this, the cells, were washed with distilled water three times, treated with the hematoxylin dye solution for 5 minutes, covered with a water-based sealing film, and imaged using a Nikon Eclipse Ti microscope (Nikon, Tokyo, Japan).

The results were analyzed by calculating the percentage of stained cells relative to the total number of cells counted.

RNA extraction and real-time polymerase chain reaction (PCR) analysis

Total RNA from lung tissues were extracted using TRIzol Reagent (Invitrogen). Subsequently, equal amounts of RNA were used to synthesize complementary deoxyribonucleic acid (cDNA) with a reverse transcriptase reagent kit (TakaRa Biotechnology, Inc., Shiga, Japan). To determine messenger ribonucleic acid (mRNA) levels, real-time PCR analysis was conducted using SYBR Premix Ex Taq (TakaRa Biotechnology, Inc., Shiga, Japan).

This method was used to assess the mRNA levels of the target gene in lung tissues.

Sample preparation and protein analysis

Lung tissues were used radio-immunoprecipitation assay (RIPA) lysis buffer. Subsequently, the tissue homogenate was subjected to centrifugation at 12,000 rpm for 15 minutes, and the resulting supernatant was carefully collected. The total protein content within the lung tissue was quantified using a bicinchoninic acid (BCA) protein analysis kit (KGP902, KeyGEN BioTECH). The supernatant was mixed with sodium dodecyl sulfate polyacrylamide gel electrophoresis (SDS-PAGE) loading buffer in a 4:1 ratio and heated in boiling water for 15 minutes to denature the proteins. Those proteins then transferred onto a polyvinylidene fluoride (PVDF) membrane. The PVDF membrane was subsequently blocked with 5% skim milk at room temperature for 2 hours to prevent nonspecific binding of antibodies. The primary antibodies [β-actin (CST, 4970S), MyD88 (CST, 4283S), interleukin-1 receptor-associated kinase (IRAK) (CST, 4504S)] were diluted in tris buffered saline tween (TBST) buffer and incubated with the membrane overnight at 4 ℃. Afterwards, the membrane was washed three times with TBST buffer to remove excess primary antibodies. The membrane was then incubated with the second antibody for 2 hours. Finally, the proteins were visualized using the ECL Key-GEN system.

Statistical analysis

The data were presented as mean ± standard error of the mean. Statistical differences among the six groups were analyzed using one-way analysis of variance (ANOVA) (with nonparametric or mixed test) with multiple comparison testing for all datasets (GraphPad Prism 8.0). A significance level of $P<0.05$ was considered statistically significant.

Results

The effect of LXRs on ABCA1 mRNA in lung after O3 exposure

Quantitative PCR was used to assess mRNA expression in

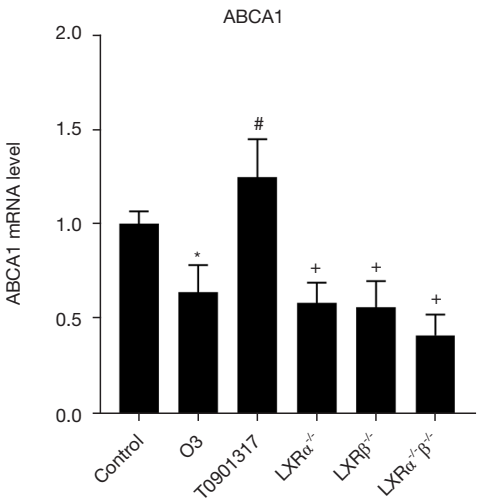

Figure 1 The effect of LXRs on ABCA1 mRNA in lung after O3 exposure. Deletion of O3 and LXR resulted in lower ABCA1 expression compared to the control group. However, mice treated with T0901317 displayed significantly higher ABCA1 levels compared to the O3 group. *, P<0.05 O3 group *vs.* Control group; #, P<0.05 T0901317 group *vs.* O3 group; +, P<0.05 LXR-deficient group *vs.* O3 group. Three independent experiments were conducted, with 5 mice in each group for each experiment. ABCA1, ATP-binding cassette transporter A1; LXRs, liver X receptors; mRNA, messenger ribonucleic acid; O3, ozone.

the whole lung. Compared to the control group, ABCA1 mRNA expression decreased significantly after O3 exposure and increased significantly following T0901317 treatment (P<0.05). LXRα$^{-/-}$/β$^{-/-}$ mice exhibited the lowest levels of ABCA1 compared to wild mice (*Figure 1*). As an essential target gene of LXRs, ABCA1 expression was suppressed by O3 exposure and LXR deletion, while LXR agonist treatment reversed the inhibition of ABCA1 in wild mice after O3 exposure.

The effect of LXRs on airway inflammatory cells and alveolar enlargement after O3 exposure

Compared with the lungs of mice in the control group, those of mice in the O3 exposed group exhibited severe emphysema and neutrophil and macrophage infiltration after O3 exposure. Mice treated with T0901317 showed a marked reduction in inflammatory cells and alveolar enlargement compared to the O3-exposed group (P<0.05). Furthermore, the LXR-deficient mice exhibited more severe airway inflammation and alveolar dilation than the wild mice after O3 exposure (P<0.05). There were no significant differences in O3-induced airway inflammation and alveolar injury among LXRα$^{-/-}$, LXRβ$^{-/-}$ and LXRα$^{-/-}$/β$^{-/-}$ mice (*Figures 2*,*3*).

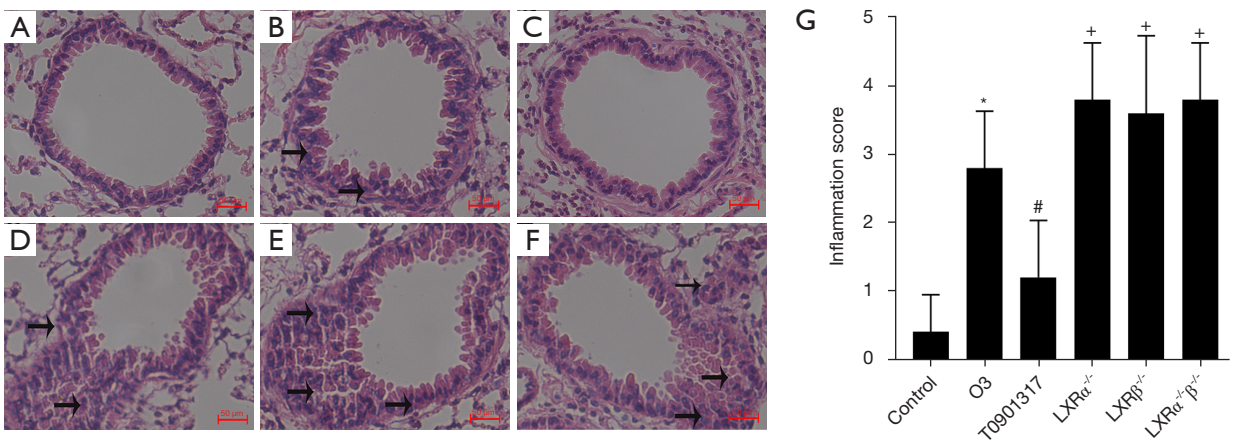

Figure 2 The effect of LXRs on airway inflammatory cells after O3 exposure. Representative HE-stained images for the (A) Control group, (B) O3 group, (C) T0901317 group, (D) LXRα$^{-/-}$ group, (E) LXRβ$^{-/-}$ group and (F) LXRα$^{-/-}$/β$^{-/-}$ group (magnification, ×200). (G) Inflammation score. The black arrows point to inflammatory cells. *, P<0.05 O3 group *vs.* Control group; #, P<0.05 T0901317 group *vs.* O3 group; +, P<0.05 LXR-deficient group *vs.* O3 group. Three independent experiments were examined (5 mice in each group of one experiment). LXRs, liver X receptors; O3, ozone; HE, hematoxylin and eosin.

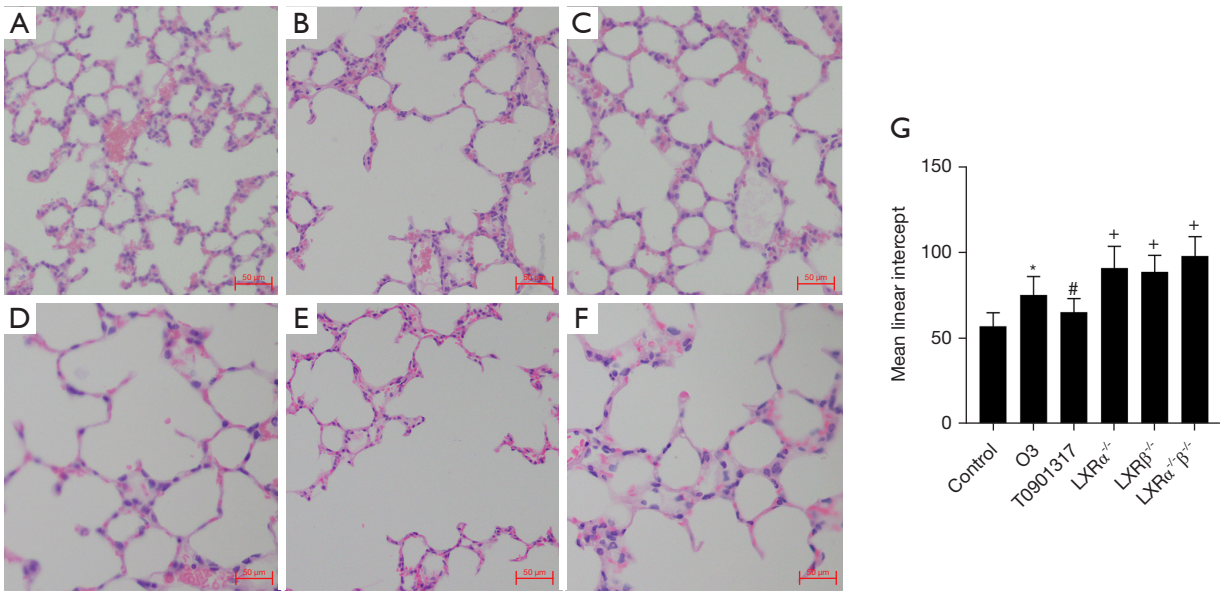

Figure 3 The effect of LXRs on alveolar enlargement after O3 exposure. (A-F) The representative HE-stained sections from the lungs of the different groups of mice (original magnification, ×200). (A) Control group, (B) O3 group, (C) T0901317 group, (D) LXRα$^{-/-}$ group, (E) LXRβ$^{-/-}$ group and (F) LXRα$^{-/-}$/β$^{-/-}$ group. (G) Quantitative analysis of the lung destruction, as represented by mean linear intercept. *, P<0.05 O3 group *vs.* control group; $^{\#}$, P<0.05 T0901317 group *vs.* O3 group; $^{+}$, P<0.05 LXR-deficient group *vs.* O3 group. Three independent experiments were examined (5 mice in each group of one experiment). LXRs, liver X receptors; O3, ozone; HE, hematoxylin and eosin.

The effect of LXRs on inflammatory cells in BALF after O3 exposure

After O3 exposure, the total number of leukocytes, predominantly consisting of macrophages, neutrophils, and lymphocytes, in BALF significantly increased compared to the control group (P<0.05). Pre-treatment with T0901317 before O3 exposure significantly reduced the number of macrophages, neutrophils, and lymphocytes in BALF (P<0.05). LXR knockout mice, on the other hand, had higher levels of these inflammatory cells compared to wild mice after O3 exposure (P<0.05). However, no significant differences in inflammatory cell counts were observed among LXRα$^{-/-}$, LXRβ$^{-/-}$ and LXRα$^{-/-}$/β$^{-/-}$ mice (*Figure 4*).

The effect of LXRs on the formation of foamy macrophages

Following O3 exposure, lipid accumulation was observed in macrophages in both wild mice and LXR knockout mice. This expression of foamy macrophage was significantly higher in absence of LXR mice (P<0.05). However, there was no difference in the percentage of foamy macrophages among the three groups: LXRα$^{-/-}$, LXRβ$^{-/-}$ and LXRα$^{-/-}$/β$^{-/-}$ mice. Treatment with T0901317 sharply reduced the proportion of foamy cells (P<0.05) (*Figure 5*).

The effect of LXRs on inflammatory cytokines in the BALF after O3 exposure

Levels of IL-6, TNF-α, and MMP9 in BALF were significantly higher in the O3-exposed group compared to the control group (P<0.05). Levels of these inflammatory cytokines were lower in the T0901317-treated group compared to the O3-exposed group (P<0.05). LXR-deficient exhibited higher levels of these cytokines in BALF than wild mice (P<0.05). No changes in inflammatory cytokine expression were observed in LXRα$^{-/-}$, LXRβ$^{-/-}$ and LXRα$^{-/-}$/β$^{-/-}$ mice (*Figure 6*).

The effect of LXRs on MyD88 and IRAK after O3 exposure

Expression of MyD88 and IRAK increased after O3 exposure in wild mice. Pre-treatment with T0901317 before O3 exposure attenuated the levels of MyD88 and IRAK in wild mice (P<0.05). LXR-deficient mice showed increased expression of MyD88 and IRAK compared to

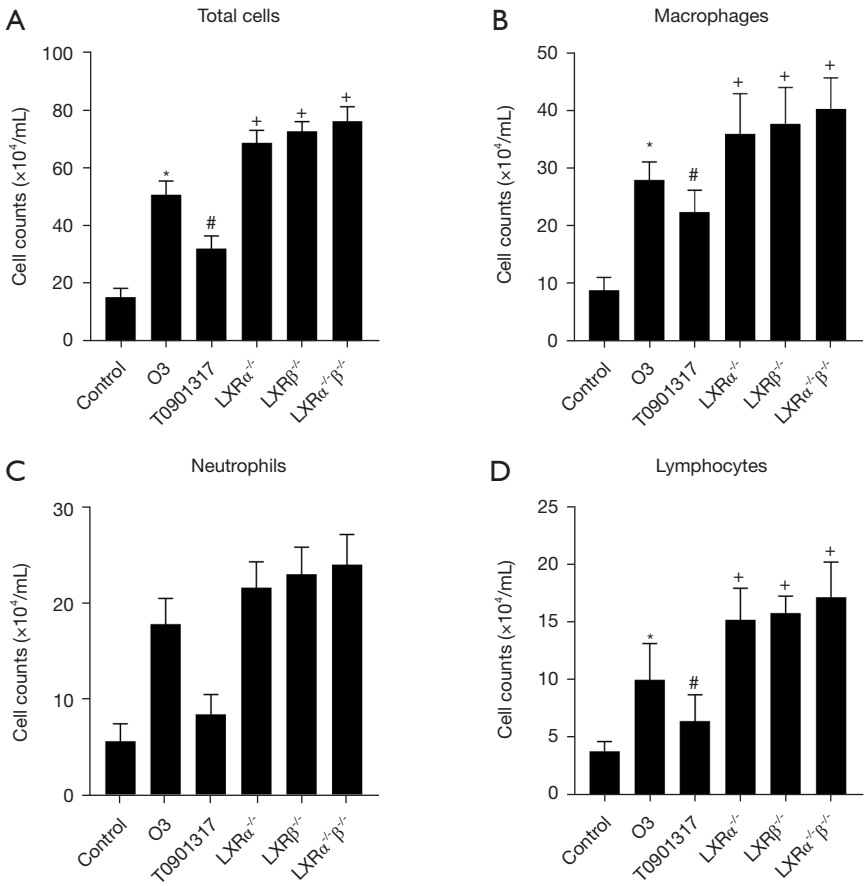

Figure 4 The effect of LXRs on inflammatory cells in BALF after O3 exposure. Total cells in BALF were counted using a cell counting plate and stained with Giemsa dye (A). Then, different cell numbers were counted at 400× magnification using a microscope (≥200 cells were counted) (B-D). *, P<0.05 O3 group *vs.* control group; #, P<0.05 T0901317 group *vs.* O3 group; +, P<0.05 LXR-deficient group *vs.* O3 group. Three independent experiments were examined (5 mice in each group of one experiment). LXRs, liver X receptors; BALF, bronchoalveolar lavage fluid; O3, ozone.

wild mice after O3 exposure (P<0.05) (*Figure 7*). Expression of MyD88 and IRAK did not differ among LXRα$^{-/-}$, LXRβ$^{-/-}$ and LXRα$^{-/-}$/β$^{-/-}$ groups.

The effect of LXRs on O3-induced submucosal fibrosis and smooth muscle hyperplasia

O3 exposure induced submucosal fibrosis (*Figure 8*) and smooth muscle hyperplasia (*Figure 9*) in wild mice. Pre-treatment with T0901317 before O3 exposure inhibited submucosal fibrosis and smooth muscle hyperplasia. LXR deficient mice exhibited more severe submucosal fibrosis and smooth muscle hyperplasia than wild mice (P<0.05). Compared to the control group, O3 stimulation increased the deposition of fibers around the bronchi, which was pronounced in LXR-deficient mice. However, T0901317 treatment significantly reduced the lung collagen levels (P<0.05) (*Figure 8A-8G*). Immunohistochemistry showed that α-SMA and MMP9 protein were highly expressed in wild mice and LXR knockout mice after O3, but this expression was attenuated by treating with the T0901317 (P<0.05). Compared to wild mice, LXR-deficient mice exhibited even higher expression of α-SMA and MMP9, although no differences were observed among LXRα$^{-/-}$, LXRβ$^{-/-}$ and LXRα$^{-/-}$/β$^{-/-}$ groups (*Figure 9A-9G*).

Discussion

O3 is considered a critical air pollutant that causes lung injuries and reduction in lung function (17). When inhaled,

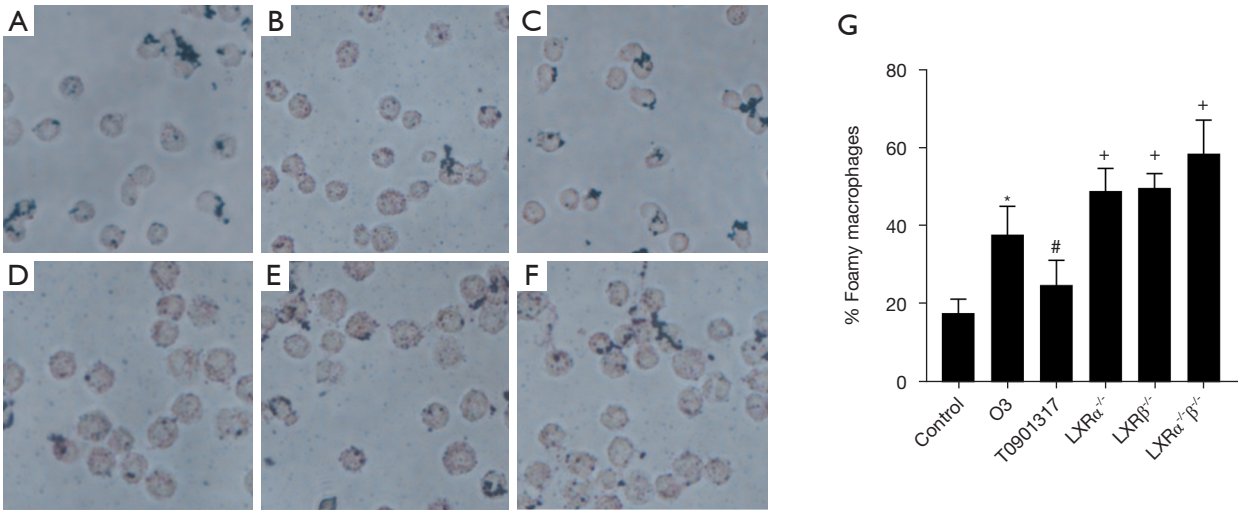

Figure 5 The effect of LXRs on the formation of foamy macrophages. The representative Oil red O staining for (A) Control group, (B) O3 group, (C) T0901317 group, (D) LXRα$^{-/-}$ group, (E) LXRβ$^{-/-}$ group and (F) LXRα$^{-/-}$/β$^{-/-}$ group (magnification, ×200). (G) Differential BALF macrophage cell count describing regular macrophages and foamy macrophages. *, P<0.05 O3 group *vs.* control group; #, P<0.05 T0901317 group *vs.* O3 group; +, P<0.05 LXR-deficient group *vs.* O3 group. Three independent experiments were examined (5 mice in each group of one experiment). LXRs, liver X receptor; O3, ozone; BALF, bronchoalveolar lavage fluid.

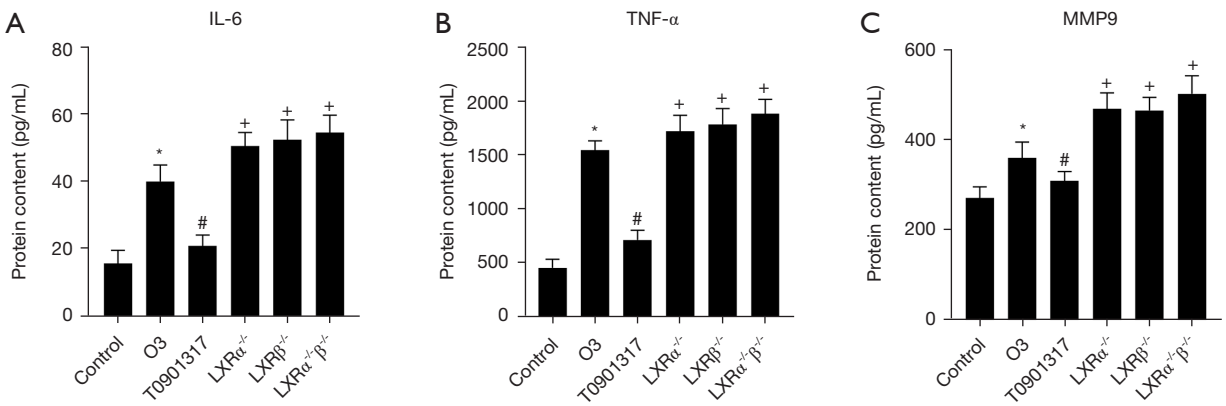

Figure 6 The effect of LXRs on inflammatory cytokines in the BALF after O3 exposure. The levels of IL-6 (A), TNF-α (B) and MMP9 (C) were determined by ELISA. *, P<0.05 O3 group *vs.* control group; #, P<0.05 T0901317 group *vs.* O3 group; +, P<0.05 LXR-deficient group *vs.* O3 group. Three independent experiments were examined (5 mice in each group of one experiment). O3, ozone; LXRs, liver X receptors; IL-6, interleukin-6; TNF-α, tumor necrosis factor-α; MMP9, matrix metallopeptidase 9; BALF, bronchoalveolar lavage fluid; ELISA, enzyme linked immunosorbent assay.

O3 reacts with the lung lining fluid to form a LOP that can activate pro-inflammatory factors, such as IL-6 and IL-8. However, the precise mechanisms through which LOP mediates airway inflammation remain unclear. Previous studies have shown that O3 oxidizes cholesterol in lung-lining fluid, leading to the generation of reactive oxysterols that exhibit pro-inflammatory effects *in vitro* (8,18). Interestingly, instead of activating LXRs, these oxysterols form adducts with LXRs and inhibit their activation by traditional agonists *in vitro* (19). Nevertheless, previous research did not investigate the impact of LXR agonists *in vivo* following O3 exposure, and the susceptibility to O3-

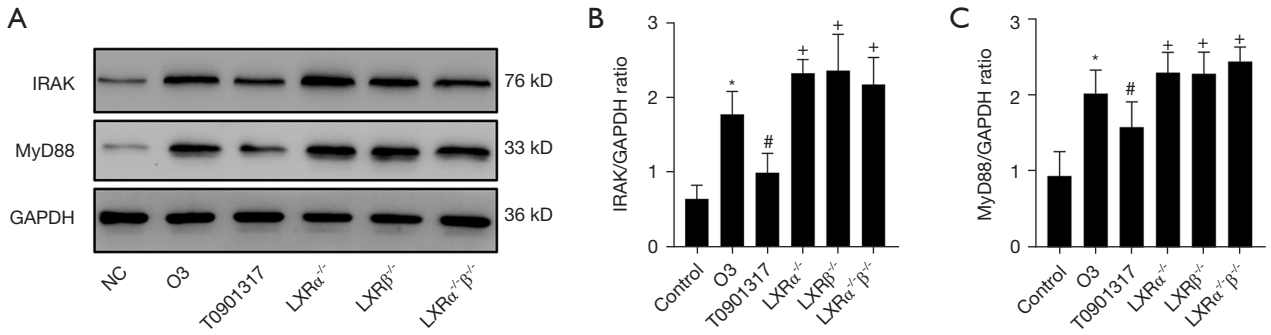

Figure 7 The effect of LXRs on O3-induced IRAK and MyD88 expression in lung. (A) IRAK and MyD88 protein expression in lung tissues of each group of mice. (B,C) Quantitative analysis of IRAK and MyD88 protein expression (n=5). *, P<0.05 O3 group *vs.* control group; #, P<0.05 T0901317 group *vs.* O3 group; +, P<0.05 LXR-deficient group *vs.* O3 group. Three independent experiments were examined (5 mice in each group of one experiment). NC, negative control; O3, ozone; LXRs, liver X receptors; IRAK, interleukin-1 receptor-associated kinase; GAPDH, glyceraldehyde-3-phosphate dehydrogenase; MyD88, myeloid differentiation primary response protein 88.

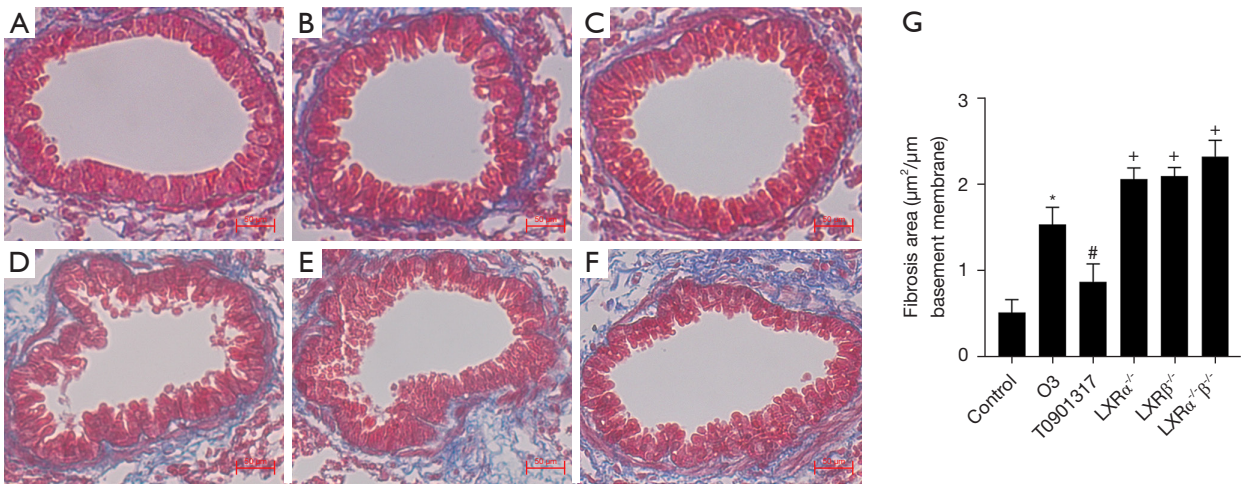

Figure 8 The effect of LXRs on O3-induced submucosal fibrosis. The representative photomicrographs demonstrate the peribranchial collagen deposition detected by Masson's trichrome staining (blue color; original magnification, ×200). (A) Control group, (B) O3 group, (C) T0901317 group, (D) LXRα$^{-/-}$ group, (E) LXRβ$^{-/-}$ group and (F) LXRα$^{-/-}$/β$^{-/-}$ group. (G) Image analysis assessing extend of Masson's trichrome staining expressed as means. *, P<0.05 O3 group *vs.* control group; #, P<0.05 T0901317 group *vs.* O3 group; +, P<0.05 LXR-deficient group *vs.* O3 group. Three independent experiments were examined (5 mice in each group of one experiment). LXRs, liver X receptors; O3, ozone.

induced acute inflammation (3-hour exposure) was only observed in LXRα$^{-/-}$. In this study, we aimed to describe the role of LXR in airway injuries and remodeling induced by intermittent O3 exposure in emphysema-like model in mice.

Myeloid differentiation primary response protein 88 (MyD88) serves as the key adaptor in inflammatory signaling pathways triggered by members of the Toll-like receptor (TLR) and interleukin-1 (IL-1) receptor families. MyD88 facilitates the connection between IL-1 receptor (IL-1R) or TLR family members and IRAK family kinases through homotypic protein-protein interactions. The activation of IRAK family kinases results in various functional outcomes, including the activation of nuclear factor-kappa B (NFκB), mitogen-activated protein kinases, and activator protein 1, positioning MyD88 as a central component in inflammatory pathways (20-22). Many studies

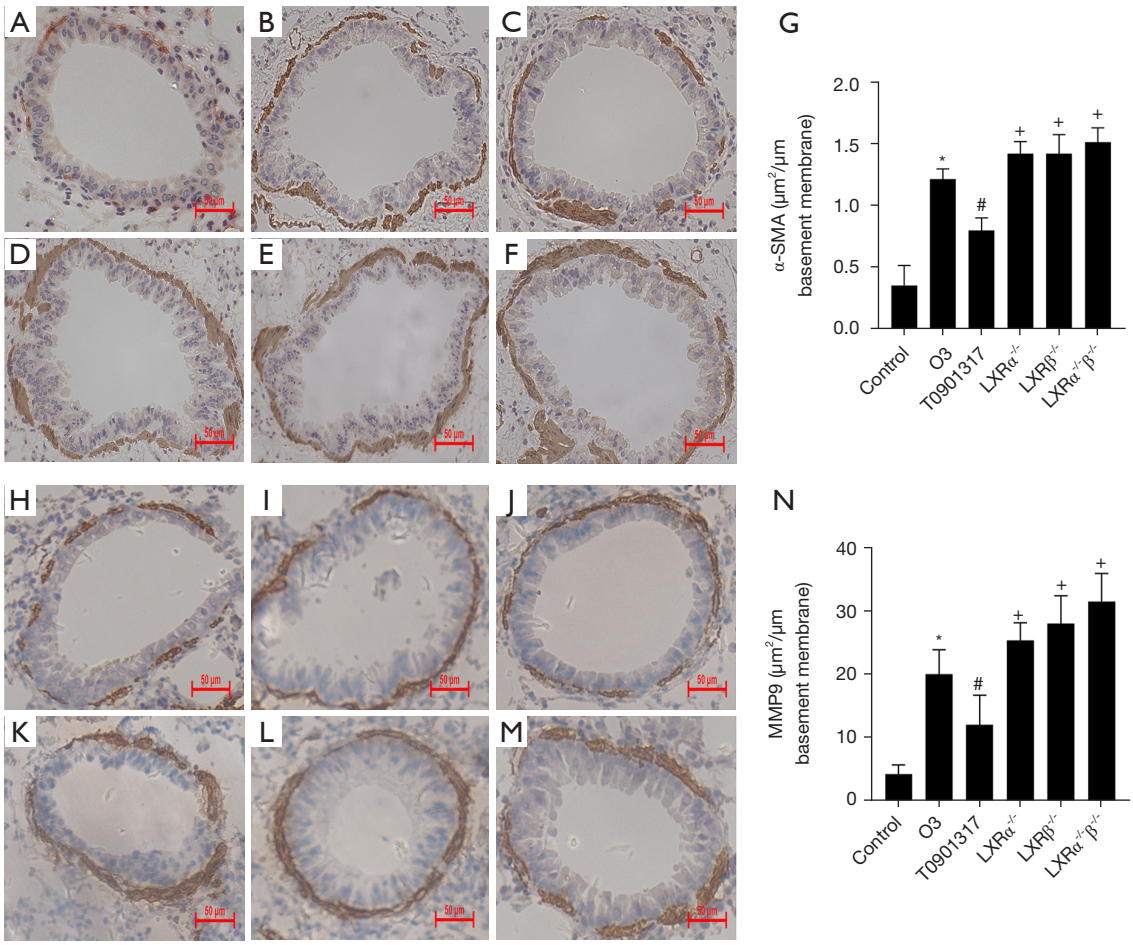

Figure 9 The effect of LXRs on O3-induced smooth muscle hyperplasia. The representative immunohistochemical staining for (A-F) α-SMA expression and (H-M) MMP9 expression. (A,H) Control group, (B,I) O3 group, (C,J) T0901317 group, (D,K) LXRα$^{-/-}$ group, (E,L) LXRβ$^{-/-}$ group and (F,M) LXRα$^{-/-}$/β$^{-/-}$ group (magnification, ×200). The area of α-SMA and MMP9 per micrometer length of basement membrane of bronchiole (G,N) were calculated. *, P<0.05 O3 group *vs.* control group; $^{\#}$, P<0.05 T0901317 group *vs.* O3 group; $^{+}$, P<0.05 LXR-deficient group *vs.* O3 group. Three independent experiments were examined (5 mice in each group of one experiment). LXRs, liver X receptors; O3, ozone; α-SMA, α-smooth muscle actin; MMP9, matrix metallopeptidase 9.

have shown that MyD88 is involved in the pathogenesis of COPD (23,24). Indoor and outdoor air pollution induces inflammatory response activating epithelial cells and alveolar macrophages via MyD88. In this study, we found that O3 exposure increased the protein expression of MyD88 and IRAK, especially in LXR deficient mice. We also found that LXR agonist can inhibit O3 induced MyD88 signaling. In addition, the experiment showed that expression of cytokines in BALF were correlated with LXR deletion or activation, So we believe that LXR may mediate O3-induced pulmonary inflammation via MyD88-IRAK signaling pathway.

LXR regulates cholesterol metabolism through ABCA1. ABCA1 is positioned on the cell membrane and facilitates the efflux of lipids, including intracellular cholesterol. This process initiates reverse cholesterol transport, which helps lower intracellular cholesterol levels. We observed that foamy macrophages increased in BALF after O3 exposure, concomitant with a significant decrease in ABCA1 expression in lung, which suggested that the cholesterol efflux capacity of macrophages was impaired by O3. The presence of foamy macrophages has been noticed in arteries of patients with atherosclerosis. The accumulation of cholesterol and ABCA1 inhibition in macrophages are associated with releasing inflammatory

mediators which are crucial for local inflammation (25). The endoplasmic reticulum (ER) is involved in protein and lipid metabolism (26), and disruption of lipid homeostasis can trigger endoplasmic reticulum stress (ERS) (27,28). Sun *et al.* discovered that ERS influences lipid catabolism in macrophages by enhancing cholesterol uptake, suppressing cholesterol efflux, and modulating the expression of associated transport proteins (29). Consequently, we propose that the emergence of foamy cells is due to the accumulation of cholesterol in macrophages, which in turn triggers ERS. Our study suggests that LXRs plays an important role in maintaining lipid homeostasis and may contribute to lung inflammation in O3 environment. Further research is needed to explore the potential involvement of ERS in this process.

COPD is characterized by irreversible fibrosis and small airway remodeling. Our findings indicate that LXRs have the capacity to mitigate O3-induced alveolar enlargement and submucosal fibrosis. Airway remodeling is closely linked to the overexpression of MMP9, an enzyme involved in extracellular matrix degradation and tissue repair (30,31). LXRs can effectively suppress the O3-induced upregulation of MMP9 levels, which may contribute to the attenuation of airway remodeling (32,33). Previous research has demonstrated that LXRs inhibit MMP9 production in macrophages through ubiquitination (34). Macrophage activation is widely recognized as a significant contributor to lung structural damage and a prominent source of MMP9 (35). Hence, LXRs may partially ameliorate airway remodeling by restraining MMP9 production in macrophages. Furthermore, epithelial-mesenchymal transition (EMT) plays a crucial role in the remodeling of small airways and the development of subepithelial fibrosis (36,37). Cigarette smoke extract and cigarette smoking can stimulate the expression of MMP9 (2,38,39), multiple studies have demonstrated a strong correlation between MMP9 and the EMT process (40-42). In our study, LXRs may have affected the process of EMT and thereby alleviated airway remodeling. In future experiments, we will strengthen relevant research to confirm this idea.

Conclusions

Our results suggest that activated LXRs confer protective effects against O3-induced lipid accumulation, airway inflammation, and remodeling in mice. The protective mechanisms of LXRs may be attributed to the activation of ABCA1 and the suppression of MyD88-IRAK pathway.

Acknowledgments

The authors acknowledge all people who contributed to this article.
Funding: This study was supported by Nanjing Medical Science and Technique Development Foundation of China (No. JQX16028 to Y.S.).

Footnote

Reporting Checklist: The authors have completed the ARRIVE reporting checklist. Available at https://jtd.amegroups.com/article/view/10.21037/jtd-23-1820/rc

Data Sharing Statement: Available at https://jtd.amegroups.com/article/view/10.21037/jtd-23-1820/dss

Peer Review File: Available at https://jtd.amegroups.com/article/view/10.21037/jtd-23-1820/prf

Conflicts of Interest: All authors have completed the ICMJE uniform disclosure form (available at https://jtd.amegroups.com/article/view/10.21037/jtd-23-1820/coif). The authors have no conflicts of interest to declare.

Ethical Statement: The authors are accountable for all aspects of the work in ensuring that questions related to the accuracy or integrity of any part of the work are appropriately investigated and resolved. The animal experiments were performed under a project license (No. SYXK [Su] 2016-0006) granted by the Animal Experiment Center of Nanjing First Hospital Affiliated to Nanjing Medical University, in compliance with guidelines established by the institution's Animal Care and Use Committee for the care and use of animals.

References

1. Nassikas N, Spangler K, Fann N, et al. Ozone-related asthma emergency department visits in the US in a warming climate. Environ Res 2020;183:109206.
2. Liu Y, Pan J, Zhang H, et al. Short-Term Exposure to Ambient Air Pollution and Asthma Mortality. Am J Respir Crit Care Med 2019;200:24-32.
3. Zhang X, Bao W, Fei X, et al. Progesterone attenuates airway remodeling and glucocorticoid resistance in a murine model of exposing to ozone. Mol Immunol 2018;96:69-77.
4. Michaudel C, Mackowiak C, Maillet I, et al. Ozone exposure induces respiratory barrier biphasic injury and inflammation controlled by IL-33. J Allergy Clin Immunol 2018;142:942-58.
5. Sun Z, Li F, Zhou X, et al. Generation of a Chronic Obstructive Pulmonary Disease Model in Mice by Repeated Ozone Exposure. J Vis Exp 2017;56095.
6. Medina-Ramón M, Zanobetti A, Schwartz J. The effect of ozone and PM10 on hospital admissions for pneumonia and chronic obstructive pulmonary disease: a national multicity study. Am J Epidemiol 2006;163:579-88.
7. Koto H, Salmon M, Haddad el-B, et al. Role of cytokine-induced neutrophil chemoattractant (CINC) in ozone-induced airway inflammation and hyperresponsiveness. Am J Respir Crit Care Med 1997;156:234-9.
8. Kafoury RM, Pryor WA, Squadrito GL, et al. Induction of inflammatory mediators in human airway epithelial cells by lipid ozonation products. Am J Respir Crit Care Med 1999;160:1934-42.
9. Kafoury RM, Hernandez JM, Lasky JA, et al. Activation of transcription factor IL-6 (NF-IL-6) and nuclear factor-kappaB (NF-kappaB) by lipid ozonation products is crucial to interleukin-8 gene expression in human airway epithelial cells. Environ Toxicol 2007;22:159-68.
10. Ulven SM, Dalen KT, Gustafsson JA, et al. LXR is crucial in lipid metabolism. Prostaglandins Leukot Essent Fatty Acids 2005;73:59-63.
11. Yang C, McDonald JG, Patel A, et al. Sterol intermediates from cholesterol biosynthetic pathway as liver X receptor ligands. J Biol Chem 2006;281:27816-26.
12. Hamilton JP, Koganti L, Muchenditsi A, et al. Activation of liver X receptor/retinoid X receptor pathway ameliorates liver disease in Atp7B(-/-) (Wilson disease) mice. Hepatology 2016;63:1828-41.
13. Smoak K, Madenspacher J, Jeyaseelan S, et al. Effects of liver X receptor agonist treatment on pulmonary inflammation and host defense. J Immunol 2008;180:3305-12.
14. Park MC, Kwon YJ, Chung SJ, et al. Liver X receptor agonist prevents the evolution of collagen-induced arthritis in mice. Rheumatology (Oxford) 2010;49:882-90.
15. Voynow JA, Fischer BM, Malarkey DE, et al. Neutrophil elastase induces mucus cell metaplasia in mouse lung. Am J Physiol Lung Cell Mol Physiol 2004;287:L1293-302.
16. Klopfleisch R. Multiparametric and semiquantitative scoring systems for the evaluation of mouse model histopathology--a systematic review. BMC Vet Res 2013;9:123.
17. Chen H, Tong H, Shen W, et al. Fish oil blunts lung function decrements induced by acute exposure to ozone in young healthy adults: A randomized trial. Environ Int 2022;167:107407.
18. Pryor WA, Wang K, Bermúdez E. Cholesterol ozonation products as biomarkers for ozone exposure in rats. Biochem Biophys Res Commun 1992;188:618-23.
19. Speen AM, Kim HH, Bauer RN, et al. Ozone-derived Oxysterols Affect Liver X Receptor (LXR) Signaling: a potential role for lipid-protein adducts. J Biol Chem 2016;291:25192-206.
20. Putra AB, Nishi K, Shiraishi R, et al. Jellyfish collagen stimulates production of TNF-α and IL-6 by J774.1 cells through activation of NF-κB and JNK via TLR4 signaling pathway. Mol Immunol 2014;58:32-7.
21. Yanagibashi T, Nagai Y, Watanabe Y, et al. Differential requirements of MyD88 and TRIF pathways in TLR4-mediated immune responses in murine B cells. Immunol Lett 2015;163:22-31.
22. Sakai J, Cammarota E, Wright JA, et al. Lipopolysaccharide-induced NF-κB nuclear translocation is primarily dependent on MyD88, but TNFα expression requires TRIF and MyD88. Sci Rep 2017;7:1428.
23. Wu Y, Gou Y, Wang T, et al. Exportin XPO6 upregulation activates the TLR2/MyD88/NF-κB signaling by facilitating TLR2 mRNA nuclear export in COPD pulmonary monocytes. Int Immunopharmacol 2024;135:112310.
24. Gao Z, Wang J, Lu G, et al. Exploration the mechanism of Shenling Baizhu San in the treatment of chronic obstructive pulmonary disease based on UPLC-Q-TOF-MS/MS, network pharmacology and in vitro experimental verification. J Ethnopharmacol 2024;324:117728.
25. Westerterp M, Murphy AJ, Wang M, et al. Deficiency of ATP-binding cassette transporters A1 and G1 in macrophages increases inflammation and accelerates

atherosclerosis in mice. Circ Res 2013;112:1456-65.
26. Borgese N, Francolini M, Snapp E. Endoplasmic reticulum architecture: structures in flux. Curr Opin Cell Biol 2006;18:358-64.
27. Chaube R, Kallakunta VM, Espey MG, et al. Endoplasmic reticulum stress-mediated inhibition of NSMase2 elevates plasma membrane cholesterol and attenuates NO production in endothelial cells. Biochim Biophys Acta 2012;1821:313-23.
28. Liu T, Duan W, Nizigiyimana P, et al. Alpha-mangostin attenuates diabetic nephropathy in association with suppression of acid sphingomyelianse and endoplasmic reticulum stress. Biochem Biophys Res Commun 2018;496:394-400.
29. Sun Y, Zhang D, Liu X, et al. Endoplasmic Reticulum Stress Affects Lipid Metabolism in Atherosclerosis Via CHOP Activation and Over-Expression of miR-33. Cell Physiol Biochem 2018;48:1995-2010.
30. Sampsonas F, Kaparianos A, Lykouras D, et al. DNA sequence variations of metalloproteinases: their role in asthma and COPD. Postgrad Med J 2007;83:244-50.
31. Salib RJ, Howarth PH. Remodelling of the upper airways in allergic rhinitis: is it a feature of the disease? Clin Exp Allergy 2003;33:1629-33.
32. Rodrigues APD, Bortolozzo ASS, Arantes-Costa FM, et al. A plant proteinase inhibitor from Enterolobium contortisiliquum attenuates airway hyperresponsiveness, inflammation and remodeling in a mouse model of asthma. Histol Histopathol 2019;34:537-52.
33. Zhang DW, Wei YY, Ji S, et al. Correlation between sestrin2 expression and airway remodeling in COPD. BMC Pulm Med 2020;20:297.
34. Castrillo A, Joseph SB, Marathe C, et al. Liver X receptor-dependent repression of matrix metalloproteinase-9 expression in macrophages. J Biol Chem 2003;278:10443-9.
35. Morissette MC, Shen P, Thayaparan D, et al. Disruption of pulmonary lipid homeostasis drives cigarette smoke-induced lung inflammation in mice. Eur Respir J 2015;46:1451-60.
36. Mahmood MQ, Sohal SS, Shukla SD, et al. Epithelial mesenchymal transition in smokers: large versus small airways and relation to airflow obstruction. Int J Chron Obstruct Pulmon Dis 2015;10:1515-24.
37. Nowrin K, Sohal SS, Peterson G, et al. Epithelial-mesenchymal transition as a fundamental underlying pathogenic process in COPD airways: fibrosis, remodeling and cancer. Expert Rev Respir Med 2014;8:547-59.
38. Agraval H, Yadav UCS. MMP-2 and MMP-9 mediate cigarette smoke extract-induced epithelial-mesenchymal transition in airway epithelial cells via EGFR/Akt/GSK3β/β-catenin pathway: Amelioration by fisetin. Chem Biol Interact 2019;314:108846.
39. Vlahos R, Wark PA, Anderson GP, et al. Glucocorticosteroids differentially regulate MMP-9 and neutrophil elastase in COPD. PLoS One 2012;7:e33277.
40. Zhu J, Wang F, Feng X, et al. Family with sequence similarity 13 member A mediates TGF-β1-induced EMT in small airway epithelium of patients with chronic obstructive pulmonary disease. Respir Res 2021;22:192.
41. Liu ZZG, Taiyab A, West-Mays JA. MMP9 Differentially Regulates Proteins Involved in Actin Polymerization and Cell Migration during TGF-β-Induced EMT in the Lens. Int J Mol Sci 2021;22:11988.
42. Peng L, Wen L, Shi QF, et al. Scutellarin ameliorates pulmonary fibrosis through inhibiting NF-κB/NLRP3-mediated epithelial-mesenchymal transition and inflammation. Cell Death Dis 2020;11:978.

Cite this article as: Yu F, Ma J, Xu K, Tang Y, Wu B, Gu W, Shi Y. Effects of liver X receptor in O3-induced airway inflammation and remodeling in mice. J Thorac Dis 2024;16(8):5005-5017. doi: 10.21037/jtd-23-1820